DYNAMIC BUCKLING OF THIN-WALLED CYLINDRICAL SHELLS SUBJECTED TO FLUCTUATING RADIAL LOADS

A. Kumar, S. Das, P. Wahi
Indian Institute of Technology Kanpur, India, 208016
Email of corresponding author: anish@iitk.ac.in

ABSTRACT

Dynamic stability of thin walled circular cylindrical shells under radially fluctuating pressure is studied in this work. Flügge-Luré-Byrne nonlinear shell theory is employed for the analysis. Stability is studied for the case of an infinitely long thin walled circular cylindrical shell. Equations of motion in axial, tangential and radial directions are obtained and the steady axisymmetric periodic solution is first obtained using the equations of motion under the assumptions of Flügge-Luré-Byrne nonlinear shell theory. Linearization about this state leads to a linear PDEs with time periodic coefficients. Galerkin projection using possible buckled modes are employed to convert the PDEs to a system of ODEs. The stability of the system of ODEs are determined using the Floquet theory. The result of this study is presented in the form of stability charts in the planes of parameters, the magnitude of the steady load, the amplitude of the variable load and the frequency of the variation. Stability is found to be lost for external pressures whose maximum value is much below the static buckling load depending on the forcing frequency. However, stability is also attained for much larger maximum external pressures for higher forcing frequencies.

INTRODUCTION

Use of thin walled circular cylindrical shells are abundant in aerospace, nuclear, oil and many other industries. In most of these applications, shells are subjected to high speed wind and hydrostatic pressures which fluctuate in time. Accordingly, a dynamic buckling and stability analysis of thin cylinders is very important for safety purposes. Wah [1] has conducted dynamic buckling analysis of thin ring subjected to impulsive load and investigated the behavior of the ring in five distinct regimes of parameters. Dynamic buckling of cylindrical shells subjected to axial impact load and base excitation with mass at top has been studied by Wei *et al.* [2], and that for a liquid filled tank with horizontal and axial excitation has been discussed by Virella *et al.* [3]. Mustafa and coworkers [4] studied the dynamic buckling of cylindrical shells submerged in liquid wherein the shell is subjected to impulsive pressure. Analysis has been done using finite element method in ABAQUS. In many applications shells have liquid at both sides (inner and outer) at different levels. Due to difference in the levels of liquid inside and outside the shells, they are subjected to radial pressures. These radial pressures give rise to dynamic loading during seismic conditions. However, investigation of the dynamic buckling and stability for such loading has not been conducted so far. Sokolov [5] investigated the response of cylindrical shells subjected to lateral, time periodic dynamic load, but did not study the stability aspect. The aim of this work is to investigate the buckling and stability behavior of cylindrical shells under fluctuating (time-periodic) radial external pressure. However, we will only consider an infinite cylinder as a first step wherein effects of the boundaries are not present and effectively the shell becomes equivalent to a thin ring.

BASIC FORMULATION

We consider a cylinder, as shown in figure 1, of radius R and thickness h. Here, h is much

smaller than R (i.e., $h \ll R$). u, v and w are the displacements of a representative point (with coordinates (R, θ, x)) on the middle surface in axial, tangential and radial directions, respectively. The middle surface is at a distance $h/2$ from both the inner and outer surfaces of the cylinder. u_1, u_2 and u_3 are the displacement components in axial, tangential and radial directions, respectively, of a point at a radial distance z away from the representative point on the middle surface. The coordinates of this point are $(\rho = R + z, \theta, x)$.

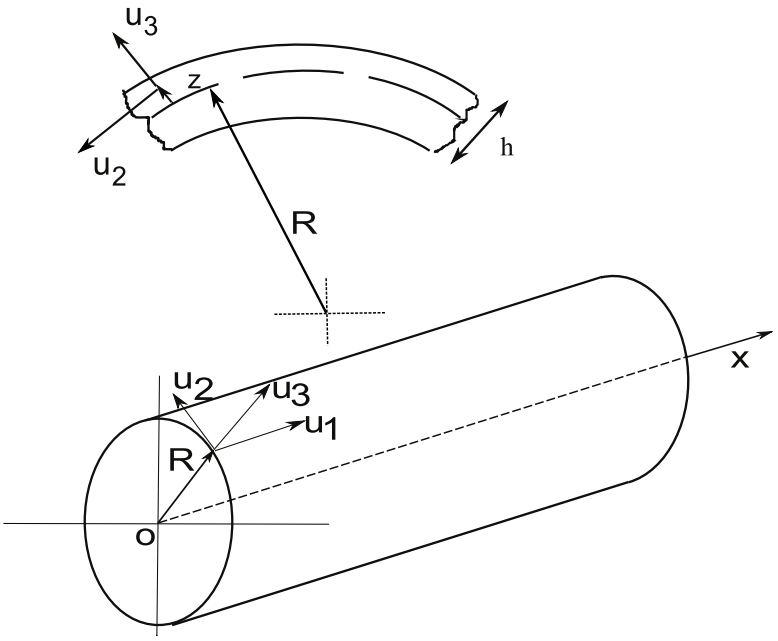

Figure 1: Schematic of a cylindrical shell showing the displacements of a point in the shell. The cylindrical coordinates (R, θ, x) are as shown.

The relations between the displacements of these two points are obtained using the assumptions of Flügge-Luré-Byrne nonlinear shell theory [6]. They are

$$u_1 = u(x, \theta, t) - z\frac{\partial w(x, \theta, t)}{\partial x}\,, \tag{1a}$$

$$u_2 = v(x, \theta, t) - \frac{z}{R}\left(\frac{\partial w(x, \theta, t)}{\partial \theta} - v(x, \theta, t)\right)\,, \tag{1b}$$

and

$$u_3 = w(x, \theta)\,. \tag{1c}$$

In the upcoming calculations $u(x, \theta, t)$, $v(x, \theta, t)$ and $w(x, \theta, t)$ are written as u, v and w respectively for simplicity. The Lagrangian strain components of a representative point on the middle surface, in cylindrical coordinate system, are denoted as $\epsilon_{xx,0}$, $\epsilon_{\theta\theta,0}$ and $\epsilon_{x\theta,0}$. Note that the components involving the radial direction are zero due to the thin shell assumption. Similarly, the nonzero strain components of the point a radial distance z away from the representative point on the middle surface are ϵ_{xx}, $\epsilon_{\theta\theta}$ and $\epsilon_{x\theta}$. The relations between the strain components of the two points are [6]

$$\epsilon_{xx} = \epsilon_{xx,0} + zk_x\,, \tag{2a}$$

$$\epsilon_{\theta\theta} = \epsilon_{\theta\theta,0} + zk_\theta\,, \tag{2b}$$

$$\epsilon_{x\theta} = \epsilon_{x\theta,0} + z k_{x\theta}\,. \tag{2c}$$

In the above, k_x, k_θ are the curvatures of the middle surface along the radial and the circumferential directions, respectively, and $k_{x\theta}$ is the torsion of the middle surface. The strain components at the middle surface are (see [6] for details)

$$\epsilon_{xx,0} = \frac{\partial u}{\partial x} + \frac{1}{2}\left(\frac{\partial w}{\partial x}\right)^2, \tag{3a}$$

$$\epsilon_{\theta\theta,0} = \frac{\partial v}{R\partial\theta} + \frac{w}{R} + \frac{1}{2}\left(\frac{\partial w}{R\partial\theta}\right)^2, \tag{3b}$$

$$\epsilon_{x\theta,0} = \frac{\partial u}{R\partial\theta} + \frac{\partial v}{\partial x} + \frac{\partial w}{\partial x}\frac{\partial w}{R\partial\theta}\,. \tag{3c}$$

The curvatures k_x , k_θ, and the torsion $k_{x\theta}$ of the representative point on the middle surface are

$$k_x = -\frac{\partial^2 w}{\partial x^2}\,, \tag{4a}$$

$$k_\theta = -\frac{\partial^2 w}{R^2\partial\theta^2} - \frac{w}{R^2}\,, \tag{4b}$$

$$k_{x\theta} = -2\frac{\partial^2 w}{R\partial x\partial\theta}\,. \tag{4c}$$

Note that the complete expressions for the curvatures and the torsion also contain nonlinear terms involving the derivatives of u and v. However, they are very small compared to radial displacement w and its derivatives, and are neglected. Accordingly, equations (4) contain terms involving w and its derivatives only. Typically, deformations are such that strains remain small and the material has been assumed to be linearly elastic. Furthermore, we consider homogeneous and isotropic material. Then, the stress components can be written as

$$\sigma_{xx} = \frac{E}{1-\nu^2}\left(\epsilon_{xx} + \nu\epsilon_{\theta\theta}\right), \quad \sigma_{\theta\theta} = \frac{E}{1-\nu^2}\left(\epsilon_{\theta\theta} + \nu\epsilon_{xx}\right), \quad \tau_{x\theta} = \frac{E}{2(1-\nu^2)}\epsilon_{x\theta},$$

where E is the modulus of elasticity and ν is the Poisson's ratio. Using these expressions for the stresses and integrating along the z (thickness) direction from $-h/2$ to $h/2$, we obtain the stress resultants which are forces per unit length and the stress moments, which are moments per unit length. The stress resultants are

$$N_x = \frac{Eh}{1-\nu^2}\left[\frac{\partial u}{\partial x} + \nu\frac{\partial v}{R\partial\theta} - \frac{\nu w}{R} + \frac{1}{2}\left(\frac{\partial w}{\partial x}\right)^2 + \frac{\nu}{2}\left(\frac{\partial w}{R\partial\theta}\right)^2\right], \tag{5a}$$

$$N_\theta = \frac{Eh}{1-\nu^2}\left[\frac{\partial v}{R\partial\theta} - \frac{w}{R} + \nu\frac{\partial u}{\partial x} + \frac{1}{2}\left(\frac{\partial w}{R\partial\theta}\right)^2 + \frac{\nu}{2}\left(\frac{\partial w}{\partial x}\right)^2\right], \tag{5b}$$

$$N_{x\theta} = \frac{Eh}{2(1+\nu)}\left[\frac{\partial v}{\partial} + \frac{\partial u}{R\partial\theta} + \frac{\partial w}{\partial x}\frac{\partial w}{R\partial\theta}\right], \tag{5c}$$

and stress moments are,

$$M_x = \frac{-Eh^3}{12(1-\nu^2)}\left[\frac{\partial^2 w}{\partial x^2} + \nu\left(\frac{\partial^2}{R^2\partial\theta^2} + \frac{w}{R^2}\right)\right], \tag{6a}$$

$$M_\theta = \frac{-Eh^3}{12(1-\nu^2)}\left[\frac{\partial^2 w}{R^2\theta^2} + \frac{w}{R^2} + \nu\frac{\partial^2 w}{\partial x^2}\right], \tag{6b}$$

$$M_{x\theta} = \frac{-EH^3}{12(1+\nu)} \frac{\partial^2 w}{R\partial x \partial \theta}. \tag{6c}$$

Equations of motion, in the cylindrical coordinates, are obtained by applying linear and angular momentum balance on an infinitesimal cylindrical element in the original configuration and, subsequently, integrating the balance equations along radial direction [6]. They are

$$\frac{\partial N_x}{\partial x} + \frac{\partial N_{x\theta}}{R\partial \theta} - \rho h \ddot{u} - c h \dot{u} = 0\,, \tag{7}$$

$$\frac{\partial N_{x\theta}}{\partial x} + \frac{\partial N_{\theta}}{R\partial \theta} - \rho h \ddot{v} - c h \dot{v} = 0\,, \tag{8}$$

$$\frac{\partial^2 M_x}{\partial x^2} + 2\frac{\partial^2 M_{x\theta}}{\partial x R \partial \theta} + \frac{\partial^2 M_{\theta}}{R^2 \partial \theta^2} + N_x \frac{\partial^2 w}{\partial x^2} + 2N_{x\theta}\frac{\partial^2 w}{\partial x R \partial \theta} + N_\theta \frac{\partial^2 w}{R^2 \partial \theta^2} - \frac{N_\theta}{R} + f = \rho h \ddot{w} + c h \dot{w} + (\rho h \ddot{u} + c h \dot{u}) \frac{\partial w}{\partial x} + (\rho h \ddot{v} + c h \dot{v}) \frac{\partial w}{R \partial \theta}\,, \tag{9}$$

where ρ is density, c is damping coefficient and f is the external radial pressure, and overdot denotes derivative with respect to time.

STABILITY ANALYSIS

In this section, we present the dynamic buckling analysis for the case of an infinitely long circular cylindrical shell. In this case, displacement along the axial direction u and all derivatives with respect to x are neglected. Thus, equation (7) is automatically satisfied. We substitute the expressions of stress resultants and moments given in equations (5) and (6) into equations (8) and (9). Upon neglecting the axial displacement and all derivatives with respect to x in the resulting expressions, the equations of motion along the tangential and the radial directions are obtained as

$$\frac{Eh}{1-\nu^2}\left[\frac{\partial^2 v}{R^2 \partial \theta^2} - \frac{\partial w}{R^2 \partial \theta} + \frac{\partial w}{R \partial \theta}\frac{\partial^2 w}{R^2 \partial \theta^2}\right] = \rho h \ddot{v} + c h \dot{v}\,, \tag{10}$$

$$\frac{-Eh^3}{12(1-\nu^2)R^4}\left(\frac{\partial^4 w}{\partial \theta^4} + \frac{\partial^2 w}{\partial \theta^2}\right) + \frac{Eh}{(1-\nu^2)R^4}\left[R\frac{\partial v}{\partial \theta} - Rw + \frac{1}{2}\left(\frac{\partial w}{\partial \theta}\right)^2\right]\frac{\partial^2 w}{\partial \theta^2} + \frac{Eh}{(1-\nu^2)R^3}\left[R\frac{\partial v}{\partial \theta} - Rw + \frac{1}{2}\left(\frac{\partial w}{\partial \theta}\right)^2\right] + f = \rho h \ddot{w} + c h \dot{w} + (\rho h \ddot{v} + c h \dot{v})\frac{\partial w}{R \partial \theta}\,. \tag{11}$$

We consider fluctuating external pressure of the form $f = F_0 + F_1 \cos \omega t$, where F_0 is the magnitude of steady pressure, F_1 is the amplitude of variable pressure, ω is the frequency of variation and t is time. Note that the loading is axisymmetric, hence the steady state solution is also axisymmetric. So all derivatives with respect to θ vanish and the final equations for steady state are

$$\rho \ddot{v} + c \dot{v} = 0\,, \tag{12}$$

$$\frac{-Eh}{(1-\nu^2)\,R^2} w + F_0 + F_1 \cos(\omega t) = \rho h \ddot{w} + c \dot{w}\,. \tag{13}$$

Steady state solution in tangential direction is assumed to be zero for simplicity. However, this does not influence the buckling and stability behavior. For radial direction steady state solution is assumed as $w(t) = w_0 + w_1 \cos(\omega t) + w_2 \sin(\omega t)$. We substitute this expression in equation (13),

bring all the terms to the left hand sides, equate the coefficients of $\cos(\omega t)$ and $\sin(\omega t)$ to zero and obtain the steady state solution in the radial direction as

$$w_0(t) = \frac{F_0 R^2(-1+\nu^2)}{Eh} + \frac{-F_1 R^2\left(-\rho\omega^2R^2+\rho\omega^2R^2\nu^2+E\right)cos(\omega t)+\omega F_1 R^4 c\left(-1+\nu^2\right)sin(\omega t)}{h\left(-2E\rho\omega^2R^2(1-\nu^2)+E^2+\rho^2\omega^4R^4(1-2\nu^2)+\rho^2\omega^4R^4\nu^4+c^2\omega^2R^4-2c^2\omega^2R^4\nu^2+c^2\omega^2R^4\nu^4\right)} \quad (14)$$

Linearzation about this state leads to two linear PDEs in v and w with time periodic coefficients. Galerkin projection using possible buckled modes are employed to convert the PDEs to a system of ODEs. Stability of the ODE system is ascertained using the Floquet theory [7]. The possible modes are

$$w(t,\theta) = \sum_{k=1}^{N} W_k(t)cos(k\theta) + \sum_{k=1}^{N} W_{N+k}(t)sin(k\theta)$$

$$v(t,\theta) = \sum_{k=1}^{N} V_k(t)cos(k\theta) + \sum_{k=1}^{N} V_{N+k}(t)sin(k\theta)$$

The mode shape corresponding to $k = 1$ is the rigid body mode [8]. Accordingly, we use the mode shape $w(t) = W_2(t)\cos(2\theta)$ and $v(t) = V_2(t)\sin(2\theta)$ (for $k = 2$). Incorporating higher order modes leads to longer computational time for the calculation of stability. However, they can be easily incorporated into the procedure and we will conduct the analysis with higher modes included in our future analysis. Also note that the mode shape for tangential displacement are related to that of radial displacement via the relation

$$\frac{\partial v}{\partial \theta} - w = 0\,.$$

This is also the condition of inextensibility of the middle surface [8]. The Galerkin projection leads to higher dimensional Mathieu-Hill equations [7] for the coefficients $W_2(t)$ and $V_2(t)$. In the following we will determine the stability of this ODE system, using Floquet multipliers [7], in the space of the various relevant parameters.

After Galerkin projection of the PDEs, the two second order ODEs that we obtain can be expressed in the following form:

$$\begin{bmatrix}\ddot{W}_2(t)\\ \ddot{V}_2(t)\end{bmatrix} + C(t)\begin{bmatrix}\dot{W}_2(t)\\ \dot{V}_2(t)\end{bmatrix} + P(t)\begin{bmatrix}W_2(t)\\ V_2(t)\end{bmatrix} = \begin{bmatrix}0\\0\end{bmatrix}\,. \quad (15)$$

The entries of the 2×2 coefficient matrices $P(t)$ and $C(t)$ are long and are provided in the appendix. We now convert the above system of second order ODEs (15) to a system of first order ODEs as

$$\dot{X} = \begin{bmatrix} 0 & 0 & 1 & 0\\ 0 & 0 & 0 & 1\\ -[P(t)] & & -[C(t)] & \end{bmatrix} X\,, \quad (16)$$

where $X = [W_2,\ V_2,\ \dot{W}_2,\ \dot{V}_2]^T$. Here, the superscript ^{T} denotes a transpose. We consider four sets of initial conditions $X^1(0) = [1,\ 0,\ 0,\ 0]^T$, $X^2(0) = [0,\ 1,\ 0,\ 0]^T$, $X^3(0) = [0,\ 0,\ 1,\ 0]^T$ and $X^2(0) = [0,\ 0,\ 0,\ 1]^T$ and solve equation (16) for each set and obtain the column vectors $X^1(T)$, $X^2(T)$, $X^3(T)$ and $X^4(T)$, which are the solutions evaluated at $t = T = 2\pi/\omega$ and T being the time period of the solution. These column vectors also constitute the 4×4 Floquet matrix $A = [X^1(T),\ X^2(T),\ X^3(T),\ X^4(T)]$. The eigenvalues of the Floquet matrix are called Floquet multipliers which predict the stability of the system of ODEs. The system is stable when all the Floquet multipliers are less than unity in magnitude and unstable when one or more of the Floquet multipliers have magnitude larger than unity. Note that the coefficient matrix in equation (16) has long time varying entries. Obtaining an analytical solution is not possible. Accordingly, we solve equation (16) numerically using MATLAB odesolver "ode45" to obtain the Floquet matrix A. We also find the eigenvalues of A (i.e., Floquet multipliers) numerically in MATLAB.

RESULTS

In figure 2 we present the stability diagram in the $F_0 - F_1$ plane for three different values of ω. Blue (dark) regions represent the stable region, i.e., in this region Floquet multipliers are all less than unity in magnitude. In the red (light) regions the system is unstable, i.e., in this region at least one Floquet multiplier has magnitude larger than unity. For large and negative values of the steady forcing F_0 the cylinder remains stable (see figure 2a). However, for a fixed internal pressure (negative F_0) as the amplitude of time varying part of the load F_1 increases, the cylinder looses stability. This case is particularly interesting because the net radial load is not always external in several applications. The static buckling load for the infinite cylinder considered in this work is $858N/m^2$. However, we observe from the unstable regions in figure 2b that for $F_0 = 225N/m^2$, the cylinder looses stability for very small positive values of F_1 for $\omega = 5$ and $\omega = 10$. The maximum load for this unstable point is much below the static buckling load. This implies that under dynamic loading the cylinder loses stability at an external pressure that is much lower than the static buckling pressure. Note that the first natural frequency of the considered cylinder is around 6 rad/sec and hence many of the attributes related to the instability under lower external pressure and stability for larger external pressures in the figures for $\omega = 5$ and $\omega = 10$ can be attributed to resonance. For a higher forcing frequency of $\omega = 15$, the unstable regimes are more or less consistent with the static one. However, we get stable regime for high values of F_0 and F_1. Hence, for higher forcing the dynamic component of the external pressure has a stabilizing effect on the first buckling mode when its magnitude becomes comparable with the mean static pressure. However, at these higher frequencies the other buckling modes might start playing a bigger role and the overall stability regime for the shell could be considerably different. For example, the second natural frequency is roughly around 16 rad/sec and at a forcing frequency of 15 rad/sec, we expect the instability regime corresponding to the second mode to have similar structure as that of the first buckling mode depicted in figure 2a. A detailed study of these aspects of the stability of the shell will be considered in our future work.

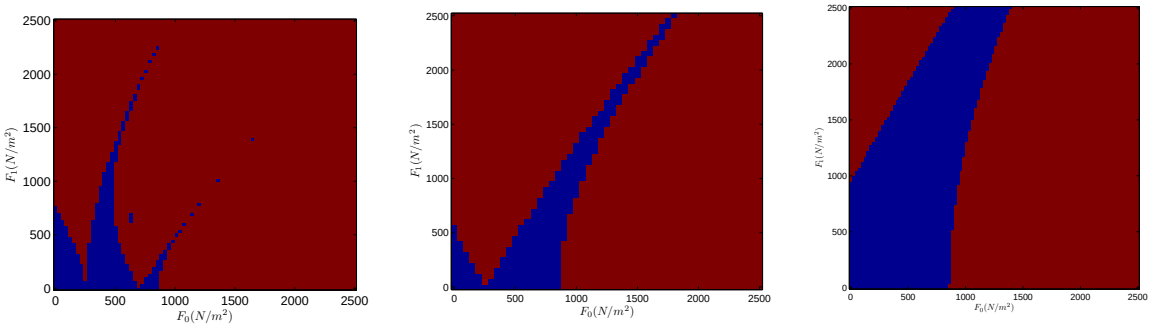

(a) (b) (c)

Figure 2: Stability diagrams in $F_0 - F_1$ plane for (a) $\omega = 5$, (b) $\omega = 10$, and (c) $\omega = 15$. The red (light) regions are unstable and the blue (dark) regions are stable. The figure on the left includes negative values of F_0. The material properties and the damping coefficient $E = 2 \times 10^11N/m^2$, $\nu = 0.3, \rho = 7680Kg/m^3$, $c = 0.1$.

In figure 3, we present the stability diagram in the $\omega - F_0$ plane for $F_1 = 400N/m^2$ and $F_1 = 600$, respectively. These results also show that the shell loses stability near the first natural frequency $\omega_{nat} = 5.98$. However, as is evident very clearly from Figure 3b that the cylinder becomes unstable for ω below ω_{nat} as well. Furthermore there is a big unstable window around $2\omega_{nat}$. The width of the unstable regime increases and the mean shifts towards lower frequencies with an increase in F_0. This is consistent with the observation that the effective stiffness of the shell reduces with an increase in the external pressure causing the natural frequencies to shift to lower values. More detailed investigation of the stability is required to better understand these diagrams.

CONCLUSION

In this work, we have investigated the stability of an infinite cylindrical shell under fluctuating (time-

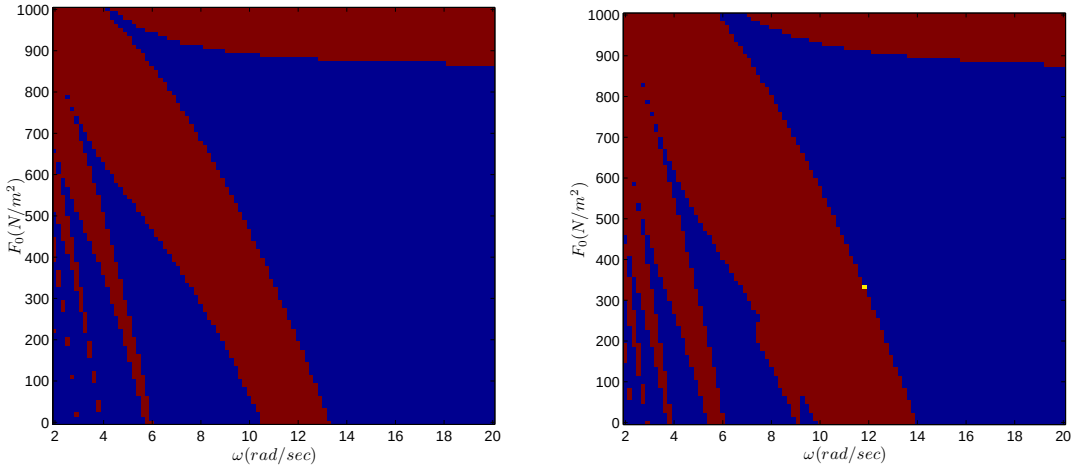

(a) (b)

Figure 3: Stability diagram in $\omega - F_0$ plane for (a) $F_1 = 400$, and (b) $F_1 = 600$. The red (light) regions are unstable and the blue (dark) regions are stable. The material properties are as mentioned in figure 2.

periodic) pressure. Stability diagrams are presented in the planes of parameters viz. the steady state pressure, the amplitude of the time varying pressure and the frequency of variation using the Floquet Multipliers for the first buckling mode. The fluctuating component of the external pressure is found to have both stabilizing as well as destabilizing effect depending on the forcing frequency. In particular, the shell has been found to loose stability for pressures whose maximum is much below the static buckling load for lower frequencies. However, for higher frequencies the shell become stable when the magnitude of the fluctuating component becomes comparable with the mean static pressure. These stability diagrams can be used as an effective tool for designing cylindrical shells that are under fluctuating pressure loading.

References

[1] T. Wah, *Dynamic buckling of thin circular ring.* International Journal of Mechanical Science , Vol 12, pp 143-155 (1970).

[2] Z. G. Wei, J. L. Yu and R. C. Batra, *Dynamic buckling of thin cylindrical shells under axial impact,* International Journal of Impact Engineering, Vol 32, pp 575-592, (2005).

[3] J. C. Virella, L. A. Godoy and L. E. Suarez, *Dynamic buckling of anchored steel tanks subjected to horizontal earthquake excitation,* Journal of Constructional Steel Research, Vol 62, pp 521-531 (2006).

[4] B. Mustafa, S. T. S. Al-Hassani and S. R. Reid, *Axisymmetric dynamic buckling of submerged cylindrical shells,* Computers and Structure, Vol 47, pp 399-405 (1992).

[5] F. A. Sokolov, *Cylindrical shell subjected to lateral dynamic pressure,* Pistol Makarova Modified U.S.S.R., Vol 45, pp 571-572.

[6] M. Amabili, *Nonlinear VIbration and Stability of Shells and Plates,* Cambridge University Press (2008).

[7] D. W. Jordan and P. Smith, *Nonlinear Ordinary Differential Equations,* Fourth Edition, Oxford University Press (2007).

[8] S. P. Timoshenko and J. M. Gere, *Theory of Elastic Stability,* Second Edition, McGraw-Hill Book Company (1963).

APPENDIX

$C(t)$ is the 2×2 matrix , whose elements are the following

$$C(t)[1,1] = (-hcR^8\rho^2\omega^4+3hc^3R^8\omega^2\nu^2-3hc^3R^8\omega^2\nu^4+hcR^4\nu^2E^2+hc^3R^8\nu^6\omega^2+2hcR^6E\rho\omega^2-3hcR^8\rho^2\omega^4\nu^4+ 3hcR^8\rho^2\omega^4\nu^2+hcR^8\nu^6\rho^2\omega^4-4hcR^6E\rho\omega^2\nu^2+2hcR^6\nu^4E\rho\omega^2-hc^3R^8\omega^2-hcR^4E^2)/((-1+\nu^2)R^4(-2E\rho\omega^2R^2+ 2E\rho\omega^2R^2\nu^2 + E^2 + \rho^2\omega^4R^4 - 2\rho^2\omega^4R^4\nu^2 rho^2\omega^4R^4\nu^4 + c^2\omega^2R^4 - 2c^2\omega^2R^4\nu^2 + c^2\omega^2R^4\nu^4)\rho h),$$

$$C(t)[1,2] = C(t)[2,1] = 0.$$

$$C(t)[2,2] = \frac{-cR^2 - cR^2\nu^2}{R^2(-1+\nu^2)\rho}$$

$P(t)$ is 2×2 matrix, whose elements are the following

$$P(t)[1,1] = (4R^3F_1\cos(\omega t)E^2 - 4R^3\nu^2F_1\cos(\omega t)E^2 - 4R^5F_1\cos(\omega t)E\rho\omega^2 + 4R^5\omega F_1 c\sin(\omega t)E + 8R^5F_1\cos(\omega t)E\rho\omega^2\nu^2 - 4R^5\nu^4F_1\cos(\omega t)E\rho\omega^2 - 8R^5\omega F_1 c\sin(\omega t)E\nu^2 + 4R^5\nu^4\omega F_1 c\sin(\omega t)E -2E^2hR^4\rho\omega^2\nu^2 + 2EhR^6\rho^2\omega^4\nu^2 - EhR^6\rho^2\omega^4\nu^4 + 2EhR^6c^2\omega^2\nu^2 - EhR^6\rho^2\omega^4 + 2E^2hR^4\rho\omega^2 - EhR^6c^2\omega^2 - 8R^5F_0E\rho\omega^2-12R^7F_0\rho^2\omega^4\nu^2+12R^7F_0\rho^2\omega^4\nu^4-12R^7F_0c^2\omega^2\nu^2+12R^7F_0c^2\omega^2\nu^4-4R^7\nu^6F_0\rho^2\omega^4-4R^7\nu^6F_0c^2\omega^2+ 2E^2h^3\rho\omega^2R^2 - Eh^3\rho^2\omega^4R^4 - Eh^3c^2\omega^2R^4 - EhR^6c^2\omega^2\nu^4 - 2E^2h^3\rho\omega^2R^2\nu^2 - Eh^3\rho^2\omega^4R^4\nu^4 + 2Eh^3c^2\omega^2R^4\nu^2 - Eh^3c^2\omega^2R^4\nu^4 + 16R^5F_0E\rho\omega^2\nu^2 - 8R^5\nu^4F_0E\rho\omega^2 - E^3h^3 + 4R^3F_0E^2 + 2Eh^3\rho^2\omega^4R^4\nu^2 - E^3hR^2 + 4R^7F_0\rho^2\omega^4 + 4R^7F_0c^2\omega^2 - 4R^3\nu^2F_0E^2)/((-1+\nu^2)R^4(-2E\rho\omega^2R^2 + 2E\rho\omega^2R^2\nu^2 + E^2 + \rho^2\omega^4R^4 - 2\rho^2\omega^4R^4\nu^2 + \rho^2\omega^4R^4\nu^4 + c^2\omega^2R^4 - 2c^2\omega^2R^4\nu^2 + c^2\omega^2R^4\nu^4)\rho h),$$

$$P(t)[1,2] = (-4E^2hR^4\rho\omega^2 + 2EhR^6\rho^2\omega^4 + 2EhR^6c^2\omega^2 - 4EhR^6\rho^2\omega^4\nu^2 + 2EhR^6\rho^2\omega^4\nu^4 - 4EhR^6c^2\omega^2\nu^2 + 2EhR^6c^2\omega^2\nu^4 + 4E^2hR^4\rho\omega^2\nu^2 + 2E^3hR^2)/((-1+\nu^2)R^4(-2E\rho\omega^2R^2 + 2E\rho\omega^2R^2\nu^2 + E^2 + \rho^2\omega^4R^4 - 2\rho^2\omega^4R^4\nu^2 + \rho^2\omega^4R^4\nu^4 + c^2\omega^2R^4 - 2c^2\omega^2R^4\nu^2 + c^2\omega^2R^4\nu^4)\rho h)$$

$$P(t)[2,1] = \frac{2E}{(R^2(-1+\nu^2)\rho)}$$

$$P(t)[2,2] = \frac{-4E}{(R^2(-1+\nu^2)\rho)}.$$